

CHARACTERIZATION OF OVERSTRENGTH FACTORS FOR BUCKLING RESTRAINED BRACES

Brandt Saxey¹, Mark Daniels²

ABSTRACT: *This paper considers the strain hardening (ω) and compression strength (β) adjustment factors for buckling-restrained braces (BRBs). Full scale test data for 39 full scale buckling restrained brace tests is presented and statistically analyzed. Ultimately backbone curves for ω and β are presented. Theoretical equations for ω and β are also presented for comparative purposes.*

KEYWORDS: Buckling restrained braces, overstrength factors, strain hardening adjustment factor, compression strength adjustment factor.

¹ Brandt Saxey, S.E., M.S. CoreBrace-Manufacturers of Buckling-Restrained Braces. Email: brandt.saxey@corebrace.com

² Mark Daniels, S.E., M.S. Mark Daniels Consulting, LLC. Email: markdaniels230@gmail.com

1 INTRODUCTION

The buckling-restrained braced frame (BRBF) has been given significant attention by designers, researchers, and manufacturers throughout the world in recent years. The short timeline in which the BRBF system has become codified and widely used in design is due to the desirable attributes the system possesses. As structural engineers increasingly employ the relatively new lateral force resisting system in projects, a desire to improve the design process to the greatest extent possible has become evident. One way to simplify the design process is to develop a statistically based BRB overstrength relationship which could be used by designers with a high level of confidence.

The purpose of this paper is to present buckling restrained brace overstrength equations. The overstrength equations are based off of a study presented at the 2011 SEAOC Convention [1] that was revisited and updated as part of the 2014 NASCC Convention [2]. Since the 2011 study, more data has been added and the overstrength equations have been statistically enhanced. The overstrength relationships presented herein represent data from thirty nine full-scale subassembly BRB tests performed at the University of California, San Diego. Data points used in the creation of the stress strain relationship were taken directly from reports prepared by the University of San Diego [3-10] and a summary table prepared by Seismic Isolation Engineering, Inc.

2 OVERSTRENGTH DISCUSSION

A unique aspect of designing a BRBF is the need for the design engineer to coordinate with BRB manufacturers to determine the *adjusted brace strength* [11]. The adjusted brace strength is a function of the axial yield force, P_{ySC} , and the overstrength factors ω (strain hardening adjustment factor) and β (compression strength adjustment factor). The adjusted brace strength in tension is identified as ωP_{ySC} ; the adjusted brace strength in compression is $\beta \omega P_{ySC}$. The overstrength factors are determined from the results of full-scale tests - preferably those including subassembly rotations of the brace. Strength beyond yield (or overstrength) measured in these tests is plotted versus the corresponding core strain in what are commonly known as “backbone curves”. These backbone curves can be used by designers to determine overstrength on a project-specific basis. These backbone curves vary from manufacturer to manufacturer (and possibly even from one brace type to another from a given manufacturer), complicating the design process and giving rise to the desire for characteristic backbone curves that

could be used for design or preliminary design. Unfortunately, codified characteristic backbone curve relationships for BRB do not currently exist. AISC 341-10 defines the tension strength adjustment factor as follows: “The strain hardening adjustment factor, ω , shall be calculated as the ratio of the maximum tension force measured from the qualification tests ... (for the expected deformations) to the measured yield force, $R_y P_{ySC}$ of the test specimen.” The term R_y is allowed to be eliminated by coupon testing. The expected deformations are the greater of the deformations that occur at two times the design story drift or 2% story drift. Since the overstrength factor ω is a measurement of material strain hardening, BRBs fabricated from similar grades of steel will have similar strain hardening adjustment factors, regardless of manufacturer, brace model, or connection type. Strain hardening is simply a property of steel. BRBs are typically fabricated from GR250 (36ksi) or similar steel plate and the strain hardening factor should be consistent with this grade of material.

The compression overstrength factor is defined in AISC 341-10 as: “The compression strength adjustment factor, β , shall be calculated as the ratio of the maximum compression force to the maximum tension force of the test specimen measured from the qualification tests...for the expected deformations.” AISC 341-10 requires β (and ω) to be larger than 1.0. Tested values below this 1.0 indicate compressive strengths less than tensile strength, which is inconsistent with BRB required performance and the AISC Seismic Provisions Commentary states that values “less than unity are not true buckling-restrained braces and their use is precluded by the provisions.” AISC Acceptance Criteria sets an upper bound value for β at 1.3.

Compressive overstrength results as a function of internal friction (imperfect debonding) and Poisson’s effect. The amount of compressive overstrength due to Poisson’s effect in a BRB can be calculated based on area relationships. Considering that the volume of the yielding core must remain the same the following relationship can be made:

$$A_0 L_0 = A_f L_f \text{ which gives, } L_f/A_0 = L_0/A_f$$

where $A_0 L_0$ are the initial area and length of the yielding core and $A_f L_f$ are the final length and area after the yielding core has strained to a given level. The strain is calculated as:

$$\varepsilon = \Delta L/L_0 = (L_f - L_0)/L_0 = L_f/L_0 - 1 = A_0/A_f - 1$$

From which the resulting area from tensile and compressive strains can respectively be calculated as:

$$A_t = A_0 / (1 + \epsilon) \quad (\text{Tension})$$

$$A_c = A_0 / (1 - \epsilon) \quad (\text{Compression})$$

The compression overstrength factor is the ratio of the compressive capacity divided by the tensile capacity. Considering only the compressive overstrength due to Poisson's effects, and noting that the yield stress cancels out of the equation, this factor, β_p , could be expressed as:

$$\begin{aligned} \beta_p &= A_0(1 + \epsilon) / A_0(1 - \epsilon) = (1 + \epsilon) / (1 - \epsilon) \\ &= (1 - \epsilon) / (1 - \epsilon) + [(1 + \epsilon) - (1 - \epsilon)] / (1 - \epsilon) \\ &= 1 + [2\epsilon / (1 - \epsilon)] \approx 1 + 2\epsilon \end{aligned} \quad (1)$$

where β_p is the compressive overstrength due to Poisson's effect and ϵ is the strain in the BRB yielding core. Equation (1) indicates that the overstrength due to Poisson effects is very nearly 2 times the level of strain greater than the tensile strength at the same level of strain. For example, if a brace strains to an amount of $\epsilon = 2.0\%$, the idealized β_p due to Poisson's effects could be very closely approximated as $1.0 + 2\epsilon$, or 1.04. This would represent the absolute minimum compression overstrength factor at this level of strain, if all other effects were completely neglected. The basis of the derivation of Equation 1 is provided by Lai & Tsai [12]

In addition to Poisson's effect, anything causing friction during the BRB compressive loading cycle can significantly increase β . For example, the yielding steel core may rub against concrete or some other material inside of the casing. Friction reducing materials may be strategically placed within the brace to reduce β . Added compressive overstrength may also be the result of a deformed steel core projection re-entering the casing during cyclic loading, or an external stabilizing mechanism, rubbing on the casing. These effects are amplified by the rotational effects associated with frame action and as such are more accurately measured from the results of subassembly tests rather than from uniaxial tests. In their study in [12] Lai & Tsai found compression overstrength factors as high as 1.30 at 2.0% strain, greatly exceeding the overstrength that would be predicted by Equation (1).

3 PRESENTATION OF DATA

3.1 SUMMARY OF DATA

This study incorporates data from 39 individual BRB full-scale subassembly test specimens, all performed at the University of California, San Diego. Data from 23 tests was obtained from CoreBrace test reports; data for 11 tests was obtained from Star Seismic test reports, and data from 5 Unbonded Brace™ tests was obtained from Seismic Isolation Engineering, Inc. The data represents BRBs ranging in yield force from 370 to 1200kN (83 to 1202 kips). Four different methods of connecting BRBs to gussets were used in testing: 15 pinned connected BRBs, 13 bolted splice plate connected BRBs, 8 bolted lug BRBs, and 3 welded BRBs. Figure 1 gives a representation of various connection types. For more details regarding connection types refer to the BRB test reports listed in the references.

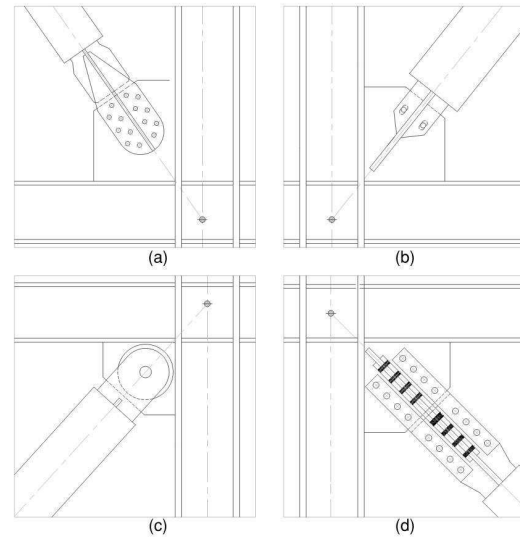


Figure 1: Schematic showing sample of BRBs with (a) bolted lug, (b) welded, (c) pinned, and (d) bolted splice plate connections. (Courtesy CoreBrace, LLC)

Data from the test reports was used to create scatter plots for ω versus strain and β versus strain, as shown in Figure 2. It is common to see this type of plot showing the β and ω terms coupled- $\beta\omega$. For the purposes of this study β has been isolated from ω .

During BRB qualification testing, multiple cycles of loading at the same level of deformation are usually performed. (AISC 341-10 requires a minimum of 2 cycles at each level of deformation.) When only 2 cycles at a given level of deformation were performed, the first data point from each set of cycles was neglected, since that cycle does not

represent a completely balanced amount of strain hardening on the tension and compression sides. For any given BRB specimen, repetitive cycles of loading beyond the first cycle produce similar values of overstrength. Therefore, for plotting purposes, when more than 2 cycles at a given level of deformation were performed, the cycles beyond the first were averaged.

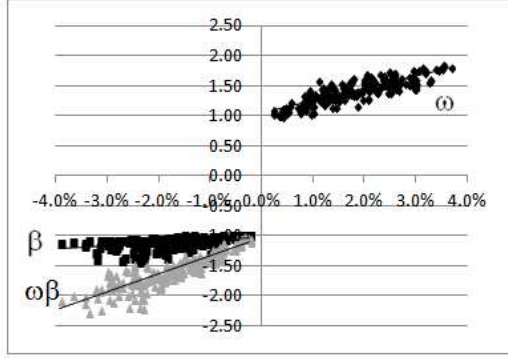


Figure 2: Scatter plot of backbone data from 39 full scale BRB tests

The strain, ϵ , presented in the scatter plots, such as shown in Figure 2, represents deformation divided by the BRB yield length. The deformation was determined from displacement measurement devices which were located slightly outside of the steel core projection, or on external collars. Designers should ensure that anticipated yielding strain can be obtained by BRBs with a high level of confidence. The levels of strains observed in the tests considered in this study ranged from yield (approximately 0.2%) to 3.9%.

Some of the UCSD test reports present ω relative to a nominal yield stress of 36ksi. For the purposes of this study, the data points were corrected to consider the yield stress based on the average value from reported coupon tests. This methodology is consistent with AISC 341-10. The average yield stress value for BRB yielding cores, based on coupon tests, ranged from 259 to 314 MPa (37.5 to 45.6 ksi).

3.2 SUMMARY OF ω

Figure 3 shows a plot of the ω data and graphically depicts a regression line that represents the best fit of this data given an amount of strain, ϵ , in the BRB yielding length. The corresponding equation for the ω regression line is:

$$\omega = 20.63\epsilon + 1.04 \quad (2)$$

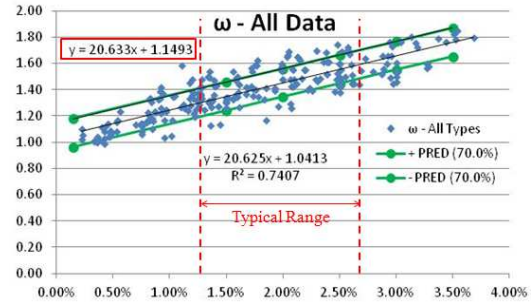


Figure 3: Strain hardening adjustment plot of backbone data from 39 full scale BRB tests

Figure 3 also shows upper and lower bound lines that represent a 70% prediction interval. A prediction interval is calculated as given in Equation 3 below:

$$\hat{y} \pm t_{n-2}^* s_y \sqrt{1 + \frac{1}{n} + \frac{(x^* - \bar{x})^2}{(n-1)s_x^2}} \quad (3)$$

where,

$$s_y = \sqrt{\frac{\sum (y_i - \hat{y}_i)^2}{n-2}}$$

In Equation 3, \hat{y} represents the value of the regression curve given in Equation (2) at a particular value of strain (x^* in Equation 3).

This level of confidence chosen for the 70% prediction interval was selected to be comparable to a mean plus one standard deviation. The lower bound prediction interval calculated from Equation 3 would not adequately capture BRB hardening characteristics. The upper bound prediction interval captures the majority of the data. The corresponding equation for the upper bound 70% prediction interval of ω is given in Equation 4:

$$\omega = 20.63\epsilon + 1.15 \quad (4)$$

The dashed lines in Figure 3 represent a typical range of design strain. The typical range is 1.30% to 2.61% corresponding to BRB ductility of 10 and 20 respectively at $F_y = 290$ MPa (42 ksi).

3.3 SUMMARY OF β

Figure 4 graphically depicts a regression line that represents the best fit of the β data given an amount of strain, ϵ , in the BRB yielding length. The corresponding equation for the β regression line is:

$$\beta = 4.96\epsilon + 1.02 \quad (5)$$

Figure 4 also shows upper and lower bound lines that represent a 70% prediction interval calculated

as given in Equation (3) and using the regression line for β given in Equation 5. The lower bound prediction interval would not adequately capture BRB compressive overstrength characteristics. The equation for the upper bound of β is:

$$\beta = 4.97\varepsilon + 1.10 \quad (6)$$

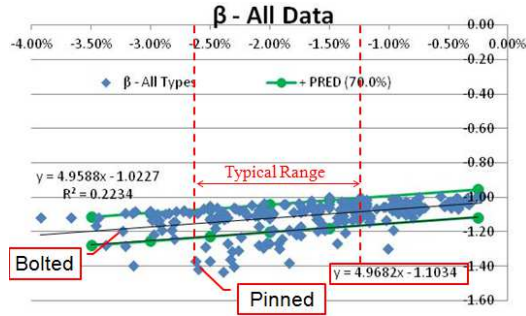


Figure 4: Compression strength adjustment plot of backbone data from 39 full scale BRB tests

The dashed lines in Figure 4 similarly show a common range of design strain. Note that the plots for β are made using negative values for compression strain with resulting negative compression overstrength factors. This has been done to result in a plot with the β values shown in the correct quadrant of a typical force displacement plot (bottom left quadrant as shown in Figure 2). However, the presented equations are given in a format requiring positive values for strain and resulting in positive values for compression overstrength factors as would typically be used in design equations.

The data for the compression strength adjustment plot is not as homogenous as it is for the tension strength adjustment plot. Table 1 summarizes the data points per connection type in the compression strength adjustment scatter plot.

Table 1: Number of data points per connection type

<u>Data Points:</u>	
Bolted	130
Pinned	86
Welded	22
Total	238

Figure 4 suggests two distinct trends. One trend consists of primarily bolted style connections; the other trend is from pinned and welded style connections. The bifurcating data sets suggests that separate compression strength adjustment curves corresponding to different brace types might be considered to avoid designing for unnecessary compressive overstrength. Otherwise, one curve that envelopes the data may be conservatively considered. It could also be noted that the majority

of the bolted braces came from a single manufacturer and the majority of the pinned braces came from another manufacturer which could also suggest that the observed differences may be related to brace manufacture. The number of data points for the welded style connections was considered statistically inadequate and are not considered separately.

Figure 5 is a compressive strength adjustment regression line for bolted style connection BRB data (pinned and welded data is included in a lighter shade). Figure 6 is a regression line for pinned data (bolted and welded data is shown in a lighter shade). The welded only plot is not shown because of the relatively small sample size.

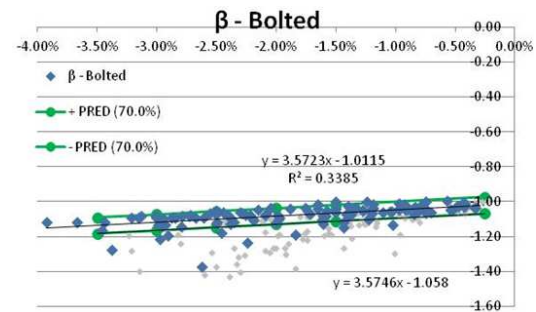


Figure 5: Compression strength adjustment plot of backbone data for bolted connection BRB tests

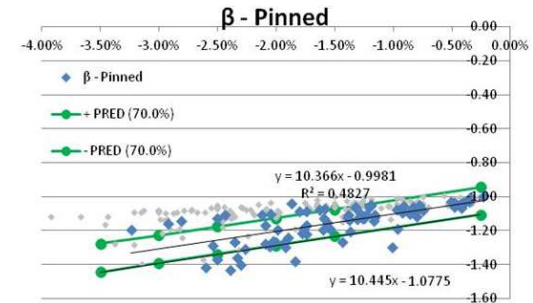


Figure 6: Compression strength adjustment plot of backbone data for pinned connection BRB tests

The equations for β_{bolted} and β_{pinned} are:

$$\beta_{\text{bolted}} = 3.57\varepsilon + 1.06 \quad (7)$$

$$\beta_{\text{pinned}} = 10.45\varepsilon + 1.08 \quad (8)$$

Examining figures 6 and 7 shows that the slope for the pinned data is steeper than the slope for the bolted data. The pinned intercept value is also larger than the bolted intercept.

4 THEORETICAL OVERSTRENGTH EQUATIONS

Theoretical equations have been developed by the authors for ω and β to be compared with the observations of the empirical data. The strain hardened capacity, P_{UT} , is shown in Figure 7 for an assumed balanced cycle (maximum compressive strain is equal to maximum tensile strain) and a linear (non-degrading) post-yield stiffness, K_p .

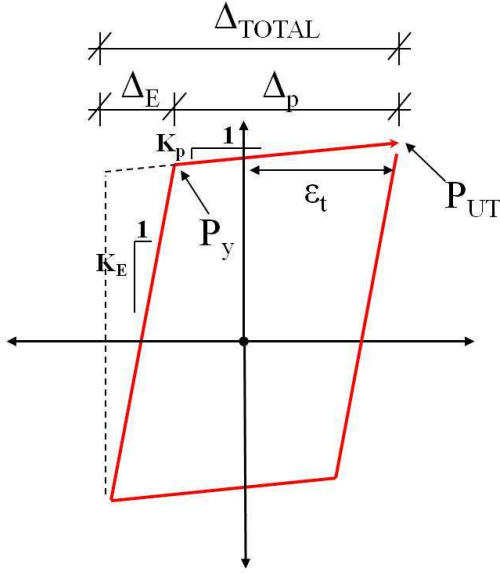


Figure 7: Diagram showing strain hardened capacity with linear pre- and post-yield stiffness.

The critical relationships of the terms in Figure 7 are given in Figure 8 and are presented in Equations (9) through (11). Considering Figure 7 and the relationships in Figure 8, the following terms can be defined:

$$K_p = \frac{P_{UT} - P_y}{\Delta_p} = \frac{P_y \omega - P_y}{\Delta_p} = \frac{P_y (\omega - 1)}{\Delta_T - \Delta_E} = \frac{P_y (\omega - 1)}{2\varepsilon_t L - P_y L / (AE)} \quad (9)$$

$$E_p = \frac{K_p L}{A} = \frac{P_y}{A} \left(\frac{\omega - 1}{2\varepsilon_t - P_y / (AE)} \right) = F_y \left(\frac{\omega - 1}{2\varepsilon_t - F_y / E} \right) \quad (10)$$

Equation 10 can be solved for the theoretical value of the strain hardening adjustment factor. Doing so yields the form given in Equation 11.

$$\omega = 1 + \frac{E_p (2\varepsilon_t - F_y / E)}{F_y} \quad (11)$$

By considering the modulus of elasticity, E , as 200 GPa (29,000 ksi), an average yield strain, F_y , of 290 MPa (42 ksi), and assuming the plastic modulus, E_p

$$\begin{aligned} \Delta_T &= \Delta_E + \Delta_p & \Delta_E &= \frac{P_y L}{AE} & \Delta_T &= 2\varepsilon_t L \\ \varepsilon_t &= \frac{\Delta_T}{2L} & \omega &= \frac{P_{UT}}{P_y} & P_{UT} &= P_y \omega \\ K_E &= \frac{AE}{L} & E &= \frac{K_E L}{A} & F_y &= \frac{P_y}{A} \end{aligned}$$

Figure 8: Critical relationships of strain hardened capacity.

is 2% of the value of the elastic modulus, E , the equation reduces to simple terms that can be solved for a given strain as given in Equation 12. (Note that Equation 12 is derived by the authors based on the imperial units and would vary slightly using the metric equivalents.)

$$\omega = 27.62\varepsilon + 0.98 \quad (12)$$

Figure 9 shows a comparison of the measured ω values and the predicted values from Equation 12. From this figure it can be seen that Equation 12 produces values lower than the 70% prediction interval at lower values of strain. The main cause of this is that Equation 12, through its derivation, produces ω values equal to 1.0 at the yield strain while the prediction interval equations overestimate this considerably at this level. Equation 12 also assumes a linear, non-degrading, post-yield stiffness while in reality a continually degrading post-yield stiffness exists, which is exhibited by the empirical data. Thus, Equation 12 over predicts ω at higher values of strain.

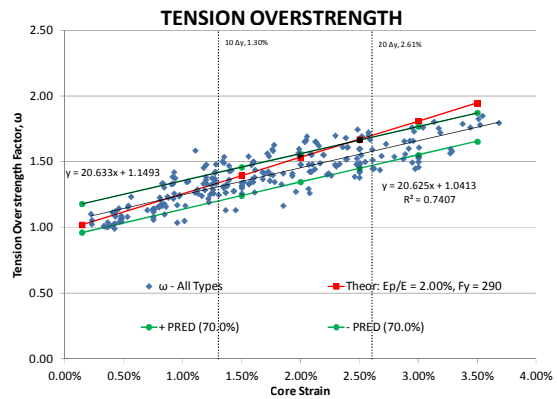


Figure 9: Comparison of tension overstrength factors: empirical data and theoretical equations.

Compressive overstrength, β must as a minimum be equal to the amount given by Equation 1. In their study, Lai and Tsai report [12] that the measured compressive overstrength is much greater than would be predicted by Equation 1, thus concluding that the effect of friction with the debonding material results for a significant amount of compressive overstrength. Figure 10 is a reproduction of a figure from the study presented in [12]. From this figure it is clear that the choice of debonding material is of considerable importance when trying to minimize the compressive overstrength.

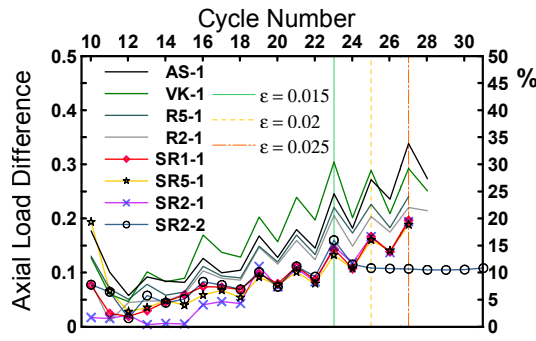


Figure 10: Axial load difference under cyclic loading. Reproduced from Lai and Tsai [12]

The information presented in Figure 10 is given in terms of axial load difference and is equivalent to the portion of the compressive overstrength factor that is greater than 1.0. For example, an axial load difference of 0.15 is equal to a β of 1.15. The research from Lai and Tsai reports that at a compressive strain of 2% the material with the lowest axial load difference (silicone rubber sheets of 2-5mm thickness) resulted in an axial load difference equivalent to a $\beta = 1 + 5\epsilon$ and that the material with the highest axial load difference (asphalt paint) resulted in an equivalent $\beta = 1 + 14\epsilon$. These equations are derived by the authors by noting the axial load difference reported by Lai and Tsai at the 2% strain level and applying these to all ranges as a function of strain. Note that both these equations for compressive overstrength factors are significantly greater than that reported in Equation 1 considering Poisson effects only.

From the results given by Lai and Tsai in [12] and observations made by the authors a convenient and nearly average value of $\beta = 10\epsilon$ for the axial load difference is selected for comparison. This value considers the effects of overstrength and some amount of friction resulting from imperfect debonding. The value of β at this level is given in Equation 13.

$$\beta = 1 + 10\epsilon \quad (13)$$

Figure 11 shows a comparison of the empirical data with the theoretical equations for β . The 70% prediction intervals are also shown. From Figure 11 it can be seen that the equation for the maximum compression overstrength ($1 + 14\epsilon$) closely matches the results of the 70% prediction interval of the pinned BRBs. The average equation ($1 + 10\epsilon$) closely matches the results of the 70% prediction interval considering all connection types together and the minimum theoretical equation ($1 + 5\epsilon$) closely matches the 70% prediction interval for the bolted only BRBs. It can also be seen that many of the bolted data points very closely approach the absolute minimum of $1 + 2\epsilon$ which considers Poisson effects only.

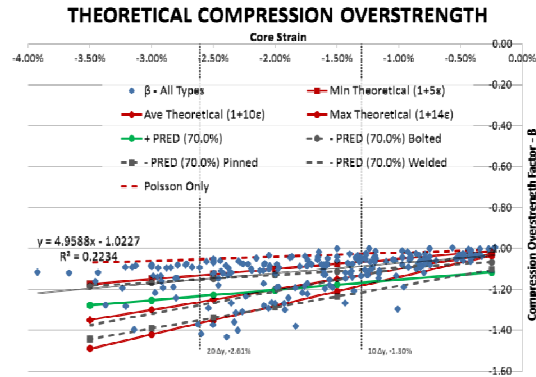


Figure 11: Comparison of compression overstrength factors: empirical data and theoretical equations.

5 CONCLUSIONS

A summary of overstrength values resulting from the presented equations are given in Table 2 for the considered design range of $10\Delta y$ - $20\Delta y$ (1.30%-2.61%).

Table 2: Summary of overstrength factors

Equation	$\omega_{10\Delta y}$	$\omega_{20\Delta y}$	$\beta_{10\Delta y}$	$\beta_{20\Delta y}$
(4) upper bound pred. int.	1.42	1.69	-	-
(12) theoretical	1.34	1.70	-	-
(7) upper bound pred. int.-bolted	-	-	1.10	1.15
(8) upper bound pred. int.-pinned	-	-	1.21	1.35
(6) upper bound pred. int.-all data	-	-	1.17	1.23
(13) theoretical	-	-	1.13	1.26

The ω values in the table show that the theoretical equation matches well with the data in the statistical analysis. The theoretical equation for ω gives lower values for tension overstrength than the 70% prediction interval equations at low levels of strain, but gives higher values than the 70% prediction interval equations at higher levels of strain.

The values in the table for β show that the theoretical equation matches well when considering all of the data. Theoretical β is conservative for the bolted data, and under conservative for the pinned data (or for that particular type of brace manufacturing).

ACKNOWLEDGEMENT

The authors would like to acknowledge CoreBrace, Nippon Steel, and Star Seismic as manufacturers of the buckling restrained braces used as the source of the data in this overstrength study. Special thanks also to Cameron Black, Keh-Chyua Tsai, and Jiun-Wei Lai. The authors would also like to thank Erin Huband for her insight and review of the statistical analysis in the study.

REFERENCES

- [1] Daniels M.: Towards Characteristic Overstrength Factors for Buckling-Restrained Braces. *SEAOC 2011 Convention Proceedings*, 2011.
- [2] Daniels M, Saxey B: Advances in Overstrength Factors for BRBs. *NASCC 2014 Convention Presentation*, Toronto, Canada
- [3] Merritt S., Uang C.M., Benzoni G., 2003a, *Subassembly Testing of CoreBrace Buckling-Restrained Braces*, Report No. TR-2003/01, University of California, San Diego, CA.
- [4] Merritt S., Uang C.M., Benzoni G., 2003b, *Subassembly Testing of Star Seismic Buckling-Restrained Braces*, Report No. TR-2003/04, University of California, San Diego, CA.
- [5] Newell J., Uang C.M., Benzoni G., 2005a, *Subassembly Testing of CoreBrace Buckling-Restrained Braces (F Series)*, Report No. TR-05/01, University of California, San Diego, CA.
- [6] Newell J., Uang C.M., Benzoni G., 2005b, *Subassembly Testing of CoreBrace Buckling-Restrained Braces (G Series)*, Report No. TR-06/01, University of California, San Diego, CA.
- [7] Benzoni G., Innamorato D., 2007, *Star Seismic Brace Tests Mercy San Juan Hospital Project*, Report No. SRMD-2007/05-rev2, University of California, San Diego, CA.
- [8] Kim D.W., Sim H.B., Uang C.M., Benzoni G., 2010a, *Subassembly Testing of CoreBrace Buckling-Restrained Braces (H Series)*, Report No. TR-09/01, University of California, San Diego, CA.
- [9] Kim D.W., Sim H.B., Uang C.M., Benzoni G., 2010b, *Subassembly Testing of CoreBrace Buckling-Restrained Braces (J Series)*, Report No. TR-09/02, University of California, San Diego, CA.
- [10] Lanning J., Uang C.M., Benzoni G., 2012, *Subassembly Testing of CoreBrace Buckling-Restrained Braces (P Series)*, Report No. TR-12/03, University of California, San Diego, CA.
- [11] American Institute of Steel Construction, 2010 AISC. 341-10, *Seismic Provisions for Structural Steel Buildings*, Chicago, IL.
- [12] Lai, J.W., Tsai, K.C. (2004), *Research and Application of Buckling Restrained Braces in Taiwan*, Proceedings, Asian-Pacific Network of Centers for Earthquake Engineering Research (ANCER), July 28-30, Honolulu, Hawaii.